

Flow of He II due to an Oscillating Grid in the Low-Temperature Limit

H. A. Nichol,¹ L. Skrbek,² P. C. Hendry,¹ and P. V. E. McClintock¹

¹*Department of Physics, Lancaster University, Lancaster LA1 4YB, United Kingdom*

²*Joint Low Temperature Laboratory, Institute of Physics ASCR and Charles University, V Holešovičkách 2, 180 00 Prague, Czech Republic*

(Received 26 August 2003; published 15 June 2004)

The macroscopic flow properties of pure He II are probed in the limit of zero temperature using an oscillating grid. As the oscillation amplitude passes a first critical threshold, the resonant frequency starts decreasing but the flow remains nondissipative. Beyond a second critical amplitude, the flow undergoes a transition to turbulence and becomes dissipative. Nonlinearity and hysteresis observed between the thresholds are attributed to a boundary layer of quantized vortices.

DOI: 10.1103/PhysRevLett.92.244501

PACS numbers: 47.37.+q, 47.15.Cb, 47.27.Cn, 67.40.Vs

Although the exotic flow properties of He II have been a subject of intensive investigation ever since the discovery of superfluidity, accumulating a vast amount of experimental data and theoretical knowledge [1,2], many important features still remain to be explained. In the limit of low velocity, He II flow is very well described in terms of Landau's two-fluid model. On exceeding a critical velocity, however, quantized vortices appear. Their presence couples the originally independent normal and superfluid velocity fields via a mutual friction. Above ~ 1.2 K, where He II contains an appreciable proportion of normal fluid, numerous investigators observed that, on exceeding a suitably defined Reynolds number, He II flow acquires an increasingly classical character: (i) the surface of a rotating bucket forms a nearly classical meniscus [3]; (ii) flow past a microsphere displays both laminar and turbulent drag [4], as well as (iii) a drag crisis [5]; (iv) the energy spectrum of turbulent He II involves an inertial range with a classical Kolmogorov roll-off exponent of $-5/3$ [6]; (v) the decay of both grid-generated and counterflow turbulence displays a classical character [7–10]. Although these features are seen over a wide range of normal fluid/superfluid density ratios, it is impossible to exclude the possibility that this classical-like behavior is caused by the presence of the viscous normal fluid. Following oscillating experiments with a tiny sphere [4] and a very thin vibrating wire [11], yielding interesting results attributable to single vortices, there is a clear call to study the *macroscopic* flow properties of He II in the $T \rightarrow 0$ limit where normal fluid is absent and pure superflow can be investigated systematically.

Our tool for performing such investigations is the thin electroformed nickel grid shown in Fig. 1. It consists of a circular membrane $2R = 8$ cm in diameter, tightly stretched on a circular mild steel carrier, mounted horizontally, equidistant from two gold-plated plane copper electrodes, each drilled with 170 holes of 2 mm inner diameter to connect the grid space to the rest of the experimental chamber. The electrodes, separated by $d = 2$ mm, are immersed in 1.5ℓ of isotopically pure liquid

^4He in an experimental cell attached to the mixing chamber of a dilution refrigerator at ~ 50 mK. The apparatus can be operated at pressures up to that of solidification at 25 bars. A static potential, typically $V_0 = 500$ V, is applied to the grid. An oscillatory potential $V_1 = V_{10} \cos \omega t$ ($V_{10} \ll V_0$) applied to the upper electrode exerts a driving force on the grid of form $f_d = 2\varepsilon_0\varepsilon_r\pi R^2 V V_1/d^2$, where ε_0 and ε_r denote, respectively, the permittivity of the vacuum and the relative permittivity of liquid ^4He . The grid can thus be considered as a driven, oscillating, membrane [12] under uniform tension. We approximate its motion as one-dimensional. Oscillations of amplitude ΔD induce a signal of amplitude $V_2 = V\Delta D/(2d)$ on the lower electrode, which can be monitored with a lock-in amplifier (which we use to investigate the low-drive linear response of the grid) or directly with a memory oscilloscope, allowing visualization of transient processes resulting from the strongly nonlinear response at higher drives. Allowing for a reduction in the induced voltage V_2 by a factor of $(1 + C_c/C)^{-1} \approx 0.065$, where $C_c \cong 700$ pF is the capacitance of the connecting cable and $C \cong 47$ pF is that between the grid and the lower

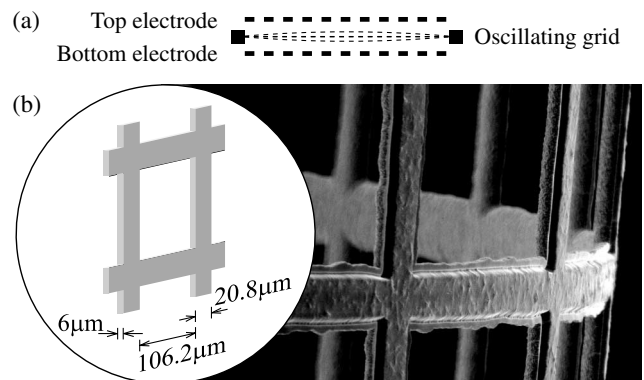


FIG. 1. Schematic drawings showing (a) a section through the electrodes and (b) the grid dimensions, together with an electron micrograph of some grid material (sample cut from the same sheet), curved in order to show it in more detail.

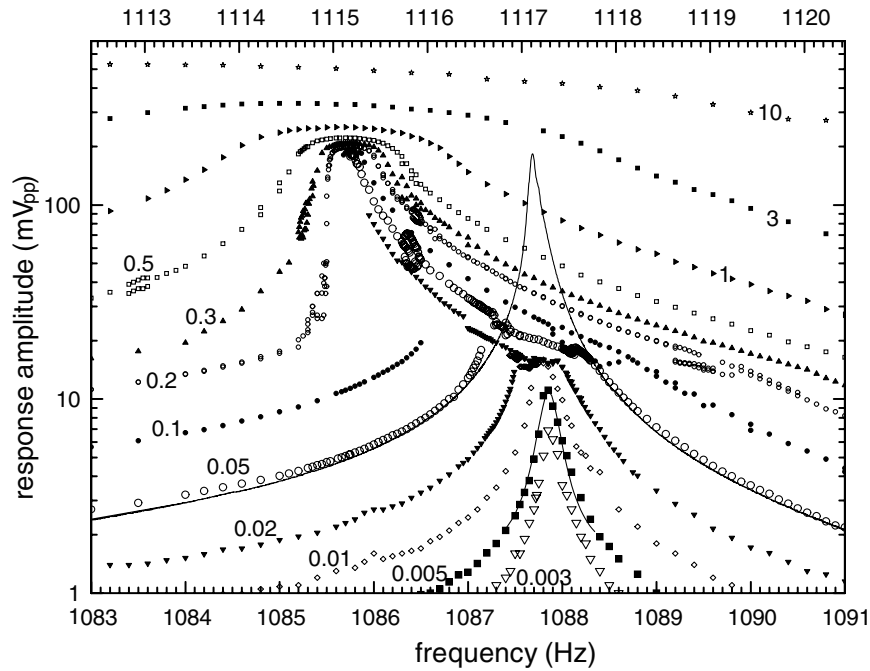


FIG. 2. Resonance curves measured at 10 bars, 50 mK, for various drive levels (in V_{pp}). The response exhibits a first critical threshold of ~ 20 mV_{pp} above which the resonant frequency shifts down with increasing drive, and a second critical threshold of ~ 200 mV_{pp} above which the frequency shift ceases but the linewidth increases dramatically. Between the thresholds, the response *on resonance* is proportional to the drive (see Fig. 3) and the flow remains nondissipative. Doubled symbols indicate places where stable beatings were observed; the lower full curve is a Lorentzian fit to the data set obtained with the $0.005 V_{pp}$ drive.

electrode, the response amplitude $|V_2|$ provides a direct measure of the amplitude and spatially averaged peak velocity $|v_g| = |\omega\Delta D|$ of the oscillating grid.

At the lowest oscillation amplitudes, the grid displays linear behavior in that its frequency response to the drive is a Lorentzian of narrow width attributable to nuisance damping, with a quality Q factor typically exceeding 5000. The resonant frequency f_{res} can be altered temporarily by a change of pressure—even if it is then returned to its original value. We attribute this to quantized vortices generated, e.g., by the jet from the filling capillary: they probably become pinned to inhomogeneities on the grid surface, and between the grid and surrounding electrodes. Moving the grid violently at high-drive amplitude, however, is found to stabilize f_{res} reproducibly, typically to within ± 0.1 Hz. Presumably, this process shakes off the longer loops of pinned vorticity.

Figure 2 shows our central experimental observation, which for the “cleaned” grid has been repeated for several pressures without appreciable change apart from a shift along the abscissa (see below). As the drive increases, the grid amplitude reaches a first critical threshold of typically 10–20 mV_{pp} (corresponding to a mean grid velocity of $0.3 < v_g^{(1)} < 0.6$ cm/s). The oscillation amplitude at resonance continues to rise linearly with the drive (cf. Fig. 3), and the flow remains nondissipative, but the resonant frequency suddenly starts decreasing and the

resonance curves acquire highly nonlinear features. If one follows, e.g., the resonance curve for the $0.05 V_{pp}$ drive down from 1091 Hz (Fig. 2) by slowly sweeping down the drive frequency, the system displays the usual nearly Lorentzian stationary response while the

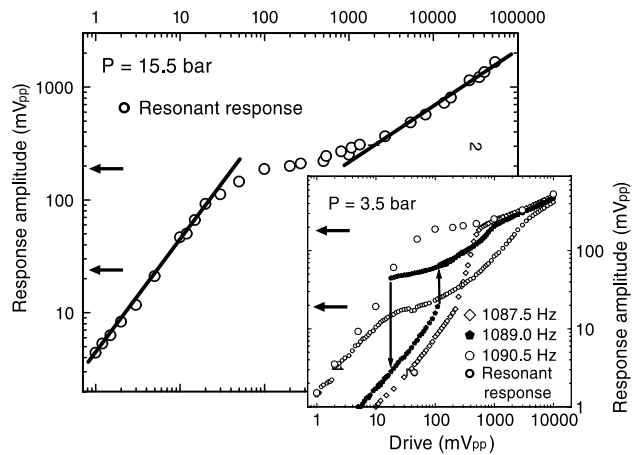


FIG. 3. Response amplitude of the grid versus the drive level at resonance (main figure) and at fixed frequencies (inset). The horizontal arrows indicate the positions of the first and second critical thresholds. For explanation of hysteresis, see text. The full lines indicate the linear and square-root responses. Note that the main figure and inset refer to different pressures.

amplitude remains below the first threshold. On further decreasing the drive frequency, the response amplitude increases more slowly above this first threshold until, shortly below 1086 Hz the amplitude suddenly collapses down to a lower stable branch. On increasing the drive frequency again from this point the system stays on the lower branch until about 1087.15 Hz, where a transition to the stable upper branch occurs. These hysteretic loops are robust to temperature increase, up to our maximum of 130 mK.

Within the hysteretic parameter range, beat phenomena are occasionally seen between two apparently stable amplitude levels, with modulation envelopes of period ~ 1 s (see, e.g., Fig. 2, drive 0.05 V_{pp}, near 1086.5 Hz); once established, they are stable on a scale of hours. Small changes of frequency modify the upper and lower amplitude levels between which beating occurs. Only with further change of the driving frequency does the beating disappear. On restoring the original frequency the response is not completely reproducible: within some small frequency range beating might not appear at all; and sometimes it reappeared only later. Despite considerable effort, we did not succeed in establishing any fully repeatable pattern or well-defined conditions for the appearance of beats. We noted that, for an oscillation amplitude exceeding the first threshold, beats occasionally appeared on the left of the resonance peak.

The fall in frequency with increasing drive (Fig. 2) reaches typically 2 Hz for all investigated pressures (see Fig. 4), ceasing at a second threshold amplitude (typically

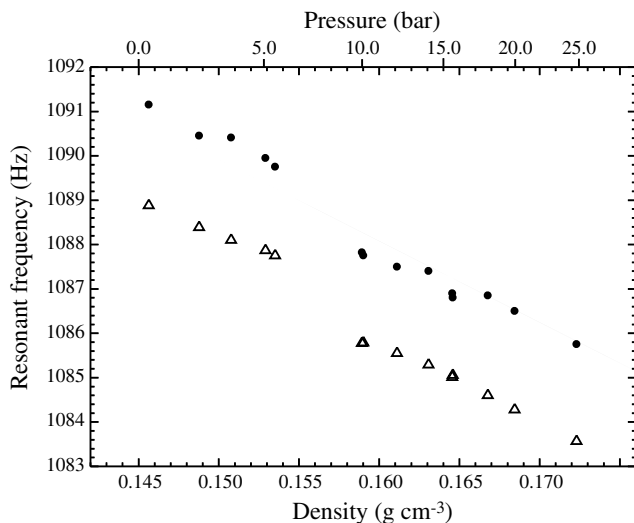


FIG. 4. Resonant frequency as a function of He II density at low drive levels (circles) and for the second critical threshold (triangles). The straight line extrapolates through the zero-density (vacuum) resonant frequency of $f_0 = 1117.2$ Hz. The corresponding pressures are marked on the upper abscissa. This shift of resonant frequency with density is due to the change in the classical hydrodynamic effective mass (see text).

200 mV_{pp} corresponding to a mean grid velocity of about $v_g^{(2)} \approx 6$ cm/s). Observation of the two well-defined resonant frequencies separated by ≈ 2 Hz is a remarkable feature of superflow that, to our knowledge, has not previously been reported. With further increase in drive, the oscillation amplitude at resonance initially remains almost constant, while the widths of the resonance curves increase rapidly (see Fig. 2). Only for drive levels exceeding by about an order of magnitude that for the second threshold does the amplitude at resonance grow again; this time approximately in proportion to the square root of the drive, as shown in Fig. 3. In this high-drive regime the linewidth increases rapidly while the resonant frequency decreases gradually. Pronounced beatings were never observed in this high-drive regime. If the oscillation amplitude is measured as a function of drive level at fixed frequency, one observes clear hysteresis within the frequency range containing the two stable branches of the grid response (Fig. 3). Beyond this range, the drive dependences are nonlinear, but without any hysteresis.

Comparison with the grid response at low temperature in vacuum (smooth curves in Fig. 2) demonstrate that the presence of the He II has two effects. First, it down shifts the low-drive resonant frequency by about 30 Hz from its vacuum value of $f_0 = (1117.2 \pm 0.05)$ Hz, depending on the pressure p in the cell (see Fig. 4). This classical effect arises from hydrodynamic enhancement of the mass M of the grid by $\Delta M_H = \beta \rho_{\text{He}}(p)M/\rho_G$, where $\rho_G = 8.902$ g cm⁻³ is the density of nickel and $\rho_{\text{He}}(p)$ is that of He II [13]. The measured f_0 and low-drive resonant frequencies yield $\beta = 3.01 \pm 0.05$. We note that, for an infinite elliptical cylinder of the same major and minor axes as the cross section of a grid bar, moving along its shorter axis, $\beta = 3$ [14]; the close agreement with our measured β suggests that our interpretation is along very much the right lines. Second, it is indeed the He II that is responsible for the observed nonlinearities [15].

We believe that the behavior of the oscillating grid ought to be understandable in terms of quantized vortices generated in He II by its motion. As one possibility, we may speculate that, on exceeding the first threshold, a “boundary layer” of vortex loops grows on the grid, thus increasing its effective mass: sufficiently small vortex loops (less than ~ 1 μ m) can distort adiabatically in the superflow field in such a way as to increase the inertia of the grid, but without adding dissipation [16]. Correspondingly, the resonant frequency shifts down and the resonance curves acquire strongly nonlinear features. Provided that the loops remain pinned, and that they do not reconnect to create free vorticity, the mass enhancement is nondissipative, as observed. We note that small mass enhancements were observed earlier for a sphere vibrating in He II above 1 K [17], but without associated critical thresholds.

It is interesting to characterize the first threshold by a superfluid Reynolds number $\text{Re}_s = U_{\text{max}}G/\kappa$, where U_{max}

stands for a peak critical flow velocity through the grid window [18], G is its linear size, and κ denotes the circulation quantum. Observed values of $Re_s \sim 10$ compare well with the critical $Re_s = UD/\kappa \approx 20$ (U is the transport velocity and D the diameter of the pipe) found as a temperature independent threshold in pipe flow of He II at much higher temperature when the flow of the normal component was inhibited by superleaks at both ends of the pipe [19]. The idea that quantized vortex loops on the surface of the grid might grow from remanent vortex lines [20], or from a “plasma” of half vortex rings [21], is supported by the following observation. While measuring the response dependence on increasing the drive amplitude at the resonant frequency, the system often encounters a nucleation problem when passing the first threshold: on some occasions the resonant response stopped growing with increasing drive level, and jumped on the response/drive curve (Fig. 3) only later. With decreasing drives this feature is absent, and the response remains proportional to the drive level.

We infer that, beyond the second critical threshold (Fig. 2), the vortex loops probably start to reconnect. Free vorticity is then shed into the liquid, corresponding to dissipation of the vibrational energy and leading to the observed increase in linewidth. Under these flow conditions, He II behaves in close analogy with a classical Navier-Stokes fluid: the square-root behavior (Fig. 3) of the resonant response as a function of drive amplitude in this range is typical of classical turbulent drag scaling, and it is, therefore, likely that this threshold marks the onset of turbulence. After leaving the grid, the quantized vorticity probably “evaporates” [22] as recently proposed in connection with turbulence in superfluid $^3\text{He-B}$ [23].

The particular challenge posed by these results is to develop a quantitative description of vortex dynamics in the macroscopic flow around the moving grid, showing how it can give rise to the observed amplitude-dependent mass enhancements and reentrant resonance curves, without dissipation [16]. But the problem also carries wider significance, and will repay careful study, because the dynamical processes in question are probably fundamental to the generation of quantum turbulence.

We are grateful to N.J. Fullwood for making the electron micrograph in Fig. 1, and to D.I. Bradley, A.M. Guénault, R.P. Haley, M. Krusius, D.G. Luchinsky, G.R. Pickett, P. Skyba, and W.F. Vinen for fruitful discussions. The research was supported by the

Engineering and Physical Sciences Research Council (U.K.) and the Czech Grant Agency under Grant No. GAČR 202/02/0251.

-
- [1] *Quantized Vortex Dynamics and Superfluid Turbulence*, edited by C. F. Barenghi, R. J. Donnelly, and W. F. Vinen (Springer, Berlin, 2001).
 - [2] J.T. Tough, in *Progress in Low Temperature Physics* (North-Holland, Amsterdam, 1982), Vol. VIII.
 - [3] D.V. Osborne, Proc. Phys. Soc. London **63**, 909 (1950).
 - [4] M. Niemetz, H. Kerscher, and W. Schoepe, J. Low Temp. Phys. **126**, 287 (2002).
 - [5] M. R. Smith, D. K. Hilton, and S.V. VanSciver, Phys. Fluids **11**, 751 (1999).
 - [6] J. Maurer and P. Tabeling, Europhys. Lett. **43**, 29 (1998).
 - [7] L. Skrbek, J. J. Niemela, and R. J. Donnelly, Phys. Rev. Lett. **85**, 2973 (2000).
 - [8] L. Skrbek, A.V. Gordeev, and F. Soukup, Phys. Rev. E **67**, 047302 (2003).
 - [9] W. F. Vinen, Phys. Rev. B **61**, 1410 (2000).
 - [10] W. F. Vinen and J. J. Niemela, J. Low Temp. Phys. **128**, 167 (2002).
 - [11] M. Morishita, T. Kuroda, A. Sawada, and T. Satoh, J. Low Temp. Phys. **76**, 387 (1989).
 - [12] M. I. Morrell, M. Sahraoui-Tahar, and P.V.E. McClintock, J. Phys. E **13**, 350 (1980).
 - [13] J. S. Brooks and R. J. Donnelly, J. Phys. Chem. Ref. Data **6**, 51 (1977).
 - [14] H. Lamb, *Hydrodynamics* (Cambridge University Press, Cambridge, 1932).
 - [15] For high-drive levels the response of the grid in vacuum also becomes nonlinear, but the nonlinearity sets in gradually and at higher amplitude than in He II.
 - [16] W. F. Vinen, L. Skrbek, and H. A. Nichol, J. Low Temp. Phys. **135**, 423 (2004).
 - [17] J. Luzuriaga, J. Low Temp. Phys. **108**, 267 (1997).
 - [18] U_{\max} is enhanced by a factor ≈ 1.43 due to the 70% grid transparency; it decreases with increasing pressure.
 - [19] M. L. Baehr, L. B. Opatowsky, and J. T. Tough, Phys. Rev. Lett. **51**, 2295 (1983).
 - [20] D. D. Awschalom and K.W. Schwarz, Phys. Rev. Lett. **52**, 49 (1984).
 - [21] F.V. Kusmartsev, Phys. Rev. Lett. **76**, 1880 (1996).
 - [22] C. F. Barenghi and D.C. Samuels, Phys. Rev. Lett. **89**, 155302 (2002).
 - [23] S. N. Fisher, A. J. Hale, A. M. Guénault, and G. R. Pickett, Phys. Rev. Lett. **86**, 244 (2001).